

# Research on Body Structural Lectotype of New-type Floating LiDAR Buoy

**Yang-yang Xue<sup>1</sup>, Pei-lin Dou<sup>1</sup>, Gang Chen<sup>2</sup>**

<sup>1</sup> School of Naval Architecture & Ocean Engineering, Jiangsu University of Science and Technology, Zhenjiang, Jiangsu Province, 212003, China

<sup>2</sup> Shanghai Waigaoqiao Shipbuilding CO., Ltd., Shanghai, 200137, China

## Abstract

Floating LiDAR (Light Detection And Ranging) buoy (FLB) systems are a flexible and particularly cost-effective alternative to the conventional meteorological mast solution, and its choice of buoy body structural styles is crucial. Based on three typical FLB systems, in this paper, four new types of FLB's type-selecting scheme are given and designed preliminarily; The intact stability of four type of FLB are studied and made a comparative analysis; By using AQWA program, the amplitude-frequency responses of four types of FLB are calculated and made a comparative analysis within the range of frequency domain; Only in this situation, considering the effect of wave and ignoring the wind and current, the four types of FLB can be analyzable for the short-term forecasts and a comparative analysis. The results show that the three-body combined buoy structural type has better comprehensive performance and we can consider it as a buoy body structural style of the new type of floating LiDAR buoy systems in the future.

**Keywords:** Floating LiDAR buoy, Intact stability, RAOs, Short-term forecast

## 1 Introduction

The measurement and collection of offshore wind data are the core components of offshore wind resource assessment and the siting of offshore wind farm. In the past time, we always built a fixed offshore meteorological (met.) mast to measure and collect offshore wind data. However, the trend of development of wind power is the exploration of deep water. And taking the difficulty of construction and the overall cost of offshore met mast into account, the traditional method can't meet the needs of current development of offshore wind industry. Hence, in the past few years, a new wind measuring system technology—Floating LiDAR (Light Detection And Ranging) Buoy (FLB) systems, based on LiDAR wind measuring technology (Pena.A., et al 2009) and ocean data buoy platform technology, had been developed. And, it was defined as a LiDAR wind measuring device that integrated in or placed on top of an ocean data buoy, offer a great potential to assess

offshore wind resources. In particular, these systems are a cost-effective and comparatively flexible alternative to fixed offshore met. Masts (Zhi-yi Liao and Heng-wen Zhang2012). Nonetheless, the motion responses of ocean data buoy platform will affect the results of wind lidar in real sea situation. A buoy body structure type designed properly with a superior performance, can minimize the motion response of buoy body platform. Therefore, the body structural lectotype of new-type floating LiDAR buoy is crucial, during its design and development process. In this paper, four new-type of FLBs' type-selecting scheme are given and designed preliminarily. We mainly focus on the stability and motion responses performance of each buoy body in waves, and ultimately choose a better buoy body structure type with excellent comprehensive performance by specific calculations and comparative analysis.




## 2 Typical offshore floating LiDAR buoy system

The Offshore Wind Accelerator (OWA) programme a Carbon Trust's flagship collaborative RD&D programme was established in 2008. And, the OWA is a joint industry project, involving nine offshore wind developers with 72% (31GW) of the UK's licensed capacity, which aims to reduce the cost of offshore wind by 10% by 2015 with the help of innovation[3]. So far, several enterprises and research institutes from Europe and North American, one after another, have launched their own floating LiDAR buoy system solutions, and also completed offshore verification test. After the long test, some solutions have contributed to obtained the appropriate commercial license.

The 'SEAWATCH' floating LiDAR buoy, integrating a ZephIR300 continuous wave wind lidar and using single point mooring method,

was developed by Fugro Oceanor company on the basis of the 'Wavescan' buoy body; The Fraunhofer IWES Wind Lidar Buoy, a developed floating-lidar system integrates a Windcubev2 lidar device in an adapted marine buoy and designed according to the navigational-light buoy LT81, was developed within the R&D project 'Offshore Messboje'; EOLOS FLS200 buoy, one new type floating LiDAR system integrating a ZephIR300 continuous wave wind lidar, was designed and developed by EOLOS solutions company. This is the three typical offshore floating LiDAR buoy system. These three buoy systems' main performance parameters and image examples are shown in Table 1. Among them, SD/MR/NH and MWT represent Suitable depth/Measurement range / Number of programmable heights and Micro-Wind Turbine respectively.

**Table 1.** Main performance parameter of three buoy systems

Name / Project	Structure type	Main dimensions	SD/MR /NH	Lidar type	Power Subsystem	Image example
Seawatch Buoy system	Disc shaped	Diameter 2.8m Height 6.1m; Δ 2.8t	>20m 10~200m 10 layers	ZephIR300	PV Panels 180W Lead acid / lithium / fuel cell	
Wind Lidar Buoy system	Disc shaped	Diameter 2.55m Height 7.2m; Δ 4.7t	≥15m 40~200m 12 layers	Windcube@v2Offshore	PV Panels 210W MWT 1.1kW AGM battery	
Eolos FLS200 Buoy system	Bowl shaped	L 4m B 4m Height 4.5m; Δ 3.0t	5~100m 10~200m 10 layers	ZephIR300M	PV Panels 1kW MWT 1.2kW Lead acid battery	

### 3 Preliminary lectotype design of floating LiDAR buoy and motion influence

#### 3.1 Preliminary lectotype design buoy body structure

Floating LiDAR buoy system is composed of buoy body, mooring system, sensor subsystem, communication subsystem, data acquisition and control subsystem and power subsystems (Jun-cheng Wang. 2013). Among them, the wind lidar device is a core component of sensor subsystem. An autonomous power subsystem, relying on wind- photovoltaic hybrid power supply technology, was designed and assembled based on micro-wind turbines, photovoltaic panels and battery banks for energy storage. Refer to the

above three floating LiDAR buoys' structure type and main technical parameters, four kinds of buoy type-selecting schemes, Buoy Lectotype Design(BLD)I,II, III, IV, were given and designed preliminarily. BLDI had a diameter of 1.5 m at the bottom of the buoy, a height of 30cm boss. The buoy body of BLDII was a vertically symmetrical round table, assembling three underwater column(3.4 m long ) and counterweight tray at the bottom of the buoy. BLDIII was composed of three small bowl-shaped floating body, belonging to triple-body combined buoy structure type and the three small floating body was arranged in the shape of an equilateral triangle, connected with strong lateral brace structure and the distance between each center of small single floating body is 2.6 m. BLDIV, belonging to four-body combined buoy structure type, consisted of four small bowl-shaped floating body, arranged in the

shape of an foursquare; the four small floating body were connected with strong lateral brace structure and the distance between each center of small single floating body is 2.25 m. Main dimensions and weight parameters of each BLD are shown in table 2; Wherein the weight of buoy does not include the mooring weight. Figure 1, 2, 3, 4 shows the overall model of BLD.



**Fig.1** BLDI model

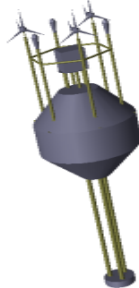


**Fig.2** BLDII model



**Fig.3** BLDIII model



**Fig.4** BLDIV model

**Table 2** Principal dimensions of four BLD

Dimensions	BLDI	BLDII	BLDIII	BLDIV
Dia.Deck (m)	3	2.55	0.9(SB)	0.875(SB)
Dia.Bottom(m)	1.5	0.74	0.6(SB)	0.6(SB)
D (m)	1.3	2.75	1	1
d (m)	0.8	4.95	0.6	0.5
$\Delta$ (ton)	3.467	4.7	3.656	3.596
W (ton)	2.443	3.604	2.645	2.464
COG <sub>z</sub> (m)	-0.18	-1.45	0.057	0.085
I <sub>xx</sub> (kgm <sup>2</sup> )	1800	14000	3730	3990
I <sub>yy</sub> (kgm <sup>2</sup> )	1800	14000	3730	3990
I <sub>zz</sub> (kgm <sup>2</sup> )	1450	1180	5830	5980

## 3.2 The effect of buoy body motion on the result of wind measurement

In the process of measuring offshore wind, translational motions and rotational motions of floating LiDAR buoy will affect the measurement of wind vector in different degree. Furthermore importing errors and reducing accuracy(M.Pitter, et al 2014). The translational motions of buoy, including sway, surge and heave, along the x, y and z axes respectively, simply add an additional motion vector to the true wind vector; The rotational motions of buoy, including roll, pitch and yaw, around the x, y and z axes respectively can induce errors in the line-of-sight speed measurement due to the tilting or yawing of the system affecting the angle between the wind vector and the measurement beam vector.

In this paper, we contrastively calculate and analyze the above four kind of preliminary design BLDs' performance, mainly from two aspects: the buoy stability and the motion responses of buoy in sea wave, and then make a better buoy structural lectotype. Among them, we focus on intact stability performance and heave, roll, pitch as well as yaw response of each buoy.

Figures and tables should be numbered sequentially in the order cited in the text and legends of the figures must be placed at proper locations in the text. Figures and tables should appear on appropriate pages and legends should appear at the bottom of the sheet. Photographs and shade drawings should be provided in glossy prints. Original figures should be suitable for direct photocopying. Captions of the figures should be placed below the appropriate figure, and captions of the table should be placed at the top of the table. Footnotes may follow tables for further information.

## 4 Theoretical Principle

### 4.1 Wave load

The wave load of small struts were calculated by using Morrison's equation(CCS 2005):

$$dF = \rho \frac{\pi D^2}{4} (C_m \dot{u} - C_A \ddot{x}) dz + \frac{1}{2} \rho C_D D |u - \dot{x}| (u - \dot{x}) dz \quad (1)$$

Where  $\rho$  is seawater density,  $C_m$  is inertia force coefficient,  $C_A$  is added mass factor,  $C_D$  is drag coefficient,  $u$  and  $\dot{u}$  are velocity and

acceleration of water particles,  $\dot{\mathbf{x}}$  and  $\ddot{\mathbf{x}}$  are velocity and acceleration of small struts. 3D potential theory is used to calculate the wave load of buoy panel model. Velocity potential  $\phi$  is consists of incident potential  $\phi_I(x, y, z, t)$ , radiation potential  $\phi_R(x, y, z, t)$  and the diffraction potential  $\phi_D(x, y, z, t)$ . Thereinto:

$$\phi_I = \frac{igA \cosh k(z+d)}{\omega \cosh kd} e^{-k(x \cos \beta + y \sin \beta)} \quad (2)$$

Where  $g$ ,  $A$  and  $K$  are acceleration of gravity, wave amplitude and wave number,  $d$  and  $\beta$  are water depth and relative wave obliquity.  $\phi_R$  and  $\phi_D$  are solved by using the boundary element method. Body surface was separated into many discrete unit elements, assuming that the velocity potential of each unit element can be expressed in node potential function of unit element node, then using collocation method and galerkin method to establish linear equations of nodal potential, and calculate the velocity potential of each node, in the end using the linearized Bernoulli equation to solve the wave force of buoy hull.

## 4.2 Frequency domain motion equation and transfer function

According to newton's law, and taking added mass, viscous and radiation damping, still water restoring force and wave exciting force into account, each buoy's frequency domain motion equations under the effect of linear regular wave were obtain(Yu Xiao-chuan, et al 2005):

$$[-\omega^2(M+A(\omega)) + i\omega(B(\omega)_p + B_p) + C + C_c]X(\omega, \beta) = F(\omega, \beta) \quad (1)$$

Where  $\omega$  is angular frequency of incident wave,  $\beta$  is relative wave obliquity,  $M$  is inertia matrix of buoy,  $A(\omega)$  is added mass matrix,  $B(\omega)_p$  is radiation damping matrix,  $B_p$  is viscous damping matrix;  $C$  is still water restoring force,  $C_c$  is restoring force matrix of mooring system,  $X(\omega, \beta)$  is motion matrix of buoy,  $F(\omega, \beta)$  is wave exciting force matrix.  $C_c$  is ignored and  $B_p$  is the 10% of critical damping in the process of calculation.

Under the effect of simple harmonic wave, the response of floating body varying with time can be written as:

$$R(\omega, \beta, t) = A \cdot \text{Re} \left[ H(\omega, \beta) e^{i(\omega t + \phi)} \right] \quad (4)$$

With the help of the transfer function  $H(\omega, \beta)$  and linear transfer function of wave force  $L(\omega, \beta)$ , the amplitude operator of response RAO can be defined as:

$$RAO(\omega) = H(\omega) L(\omega) \quad (5)$$

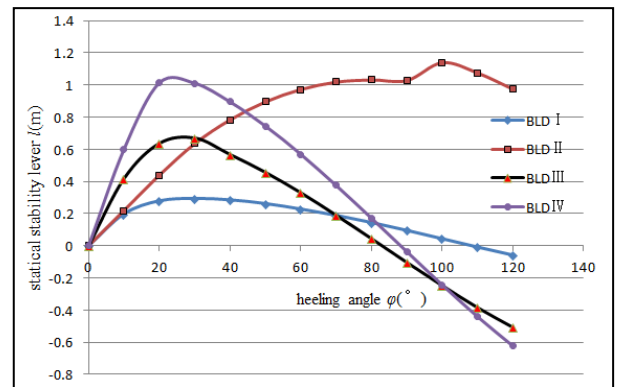
## 5 The buoy body stability calculation and contrast analysis

Floating LiDAR buoy should work in the corresponding sea area for long term. It may appear capsizing case, when encountering inclement sea-state conditions. So the pros and cons of buoy stability is very important to buoy structural lectotype. At present, there is no specific rule with regard to buoy stability in domestic. Buoy stability checking is mainly based on "Technical Regulation for Statutory Survey of Seagoing Ships". After finishing the intact stability calculation of the above four BLD, according to the aforementioned rules, each BLD's calculation results were checked and compared.

With regard to Seagoing Ships' stability, the aforementioned rules stipulated below (Zhen-bang Sheng, Ying-zhong Liu. 2009): (1) Disappear Angle of static stability  $\phi_v$  should be greater than 55°; (2) Initial stability high  $\overline{GM}$  should not be less than 0.15 m; (3) The heeling Angle  $\phi = 30^\circ$  of static stability arm  $l_{\phi=30^\circ}$  shall be not less than 0.2 m; (4) the maximum righting lever of the heeling angle  $\phi_{max}$  should not be less than 30°; Among them, when the ratio of the breadth and depth of ship is greater than 2,  $\phi_{max}$  can be smaller than the value stipulated in (4)  $\delta\phi$ .

After calculation and statistics, the wind heeling lever of four BLD respectively is 0.073m, 0.605m, 0.068m as well as 0.063m. Moreover, the static/dynamic stability curves of four BLD and the calculation of minimum upsetting lever are shown in Figure 5 and 6; Initial stability high and specific numerical statistical for static stability lever as shown in Table 3.

Fig.5 Static stability curves for four BLD





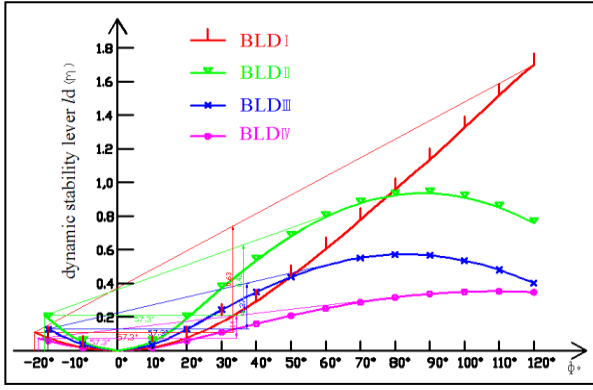


**Fig.6** Dynamic stability curves & Min. upsetting lever calculation for four BLD

**Table 3** Stability parameter statistics

Stability para.	BLDI	BLDII	BLDIII	BLDIV
$\overline{GM}(m)$	1.083	1.259	2.468	3.779
$l_{\varphi=30^\circ}(m)$	0.295	0.635	0.644	1.011
$l_m(m)$	0.295	1.142	0.671	1.052
$\varphi_m(^{\circ})$	@30°	@101°	@31°	@24°
K	1.92	10.41	3.94	6.69

As shown in Figure 5, 6 and table 3, the intact stability high  $\overline{GM}$  of four BLDs can meet the requirements of aforementioned rules, and in numerical,  $\overline{GM}$  of BLDIV is the largest, followed by BLDIII. The heeling Angle  $\varphi = 30^\circ$  of static stability arm of four BLDs can meet the requirements of aforementioned rules and  $l_{\varphi=30^\circ}$  for BLDIV is the largest and followed by BLD III in numerical. Disappear Angle of static stability of four BLDs are greater than  $80^\circ$ , meeting the requirements of aforementioned rules. In term of maximum righting lever of the heeling angle  $\varphi_{max}$ , BLD I, II and III all meet the requirements of rules, but the value of BLD IV is slightly smaller than rule's requirement and need for adjusting buoy stability. Since BLD II has a deeper draft structural features, its static and dynamic stability curve are relatively unique and quite different with the other three BLD. The stability criterion numeral K of four BLDs are greater than 1, meeting the requirements of the specification, and there is a large surplus value.

After comparative analysis, the results show that intact stability of BLDIV is the best, BLDIII followed. Moreover, the stability criterion numeral K of four BLDs has a large surplus value.

## 6 Frequency domain calculation and comparative analysis

Coordinate selection: Z axis, vertical upward, coincide exactly with the central axis of each BLD buoy model and zero point is the intersection point of central axis and waterline plane. The coordinate origin of X and Y axis is located at the center of each BLD buoy model. The zero point of BLDI and II is located at the center of its buoy model. Coordinate origin for BLD III is located in the center of the circumcircle of triangle that composed of three center point of small floating body; BLDIV's coordinate origin is located in the center of the circumcircle of square that composed of four center point of small floating body. BLD III Model is only symmetrical about X-axis, while, BLDI, II and IV are all symmetrical about X-axis and Y-axis. We focus on the main floating body portion of each buoy, while ignoring the buoy tower and the instrument cabin above buoy deck in the process of establishing hydrodynamic model. The hydrodynamic models and coordinate of each BLD are shown in Figure 7, 8, 9 and 10.

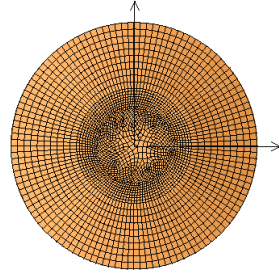


**Fig. 7** BLDI

hydrodynamic model

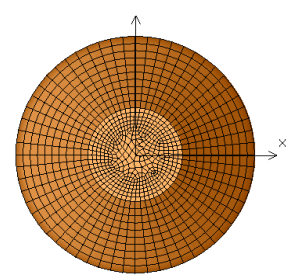


**Fig. 8** BLDII

hydrodynamic model

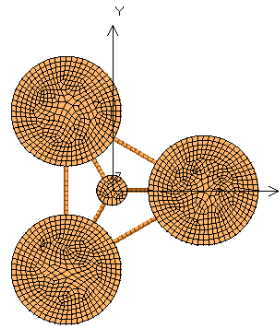


**Fig. 9** BLDI

hydrodynamic model

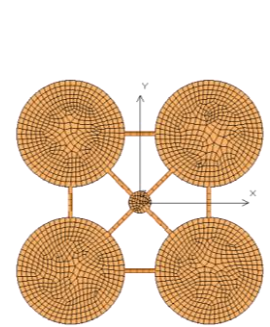


**Fig.10** BLDII

hydrodynamic model

In the process of frequency domain calculation and analysis, the operating depth of each buoy is 50 meter; Wave frequency range is 0.1~5rad/s with 0.1rad/s frequency interval; As well as wave application direction range is  $-180^{\circ} \sim 180^{\circ}$ . And finally, the response-amplitude operators (RAOs) of each buoy within the frequency domain limits are calculated. So there are three RAO graph of heave, roll and pitch are shown in Figure 11, 12 and 13 respectively. From BT1\_D to BT4\_D represent BLDItoIV respectively.

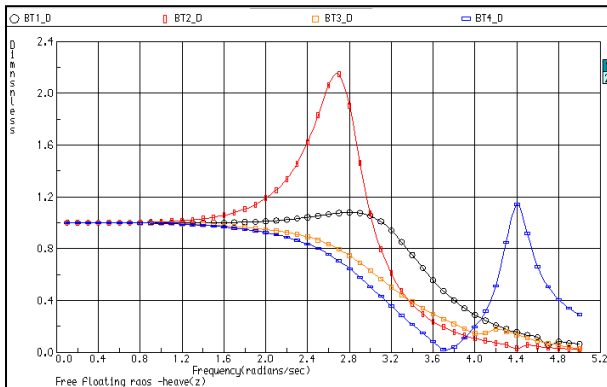


**Fig. 11** Heave RAO

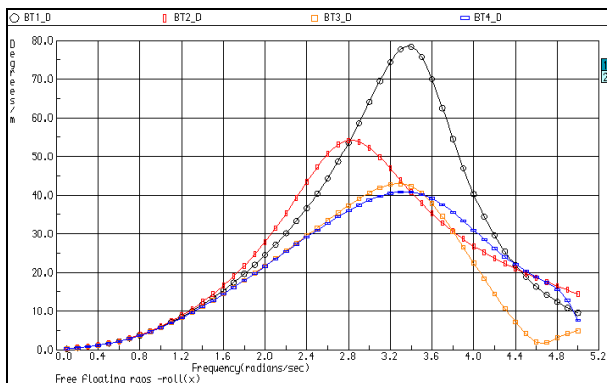


**Fig. 12** Roll RAO

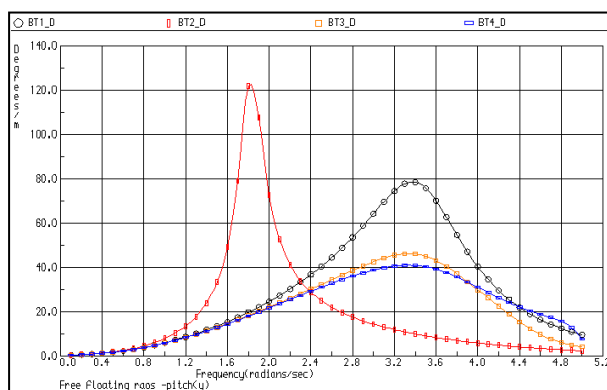


**Fig. 13** Pitch RAO

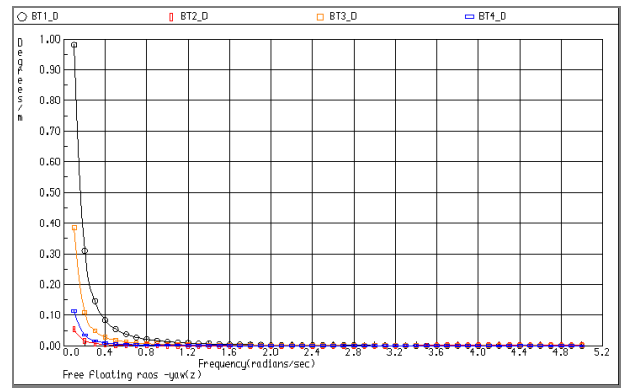


**Fig. 14** Yaw RAO

As shown in Figure 11, when the wave frequency is less than 2.2 rad / s, the heave RAO curve trend of BLDI is flat; and when it increases to 2.8 rad/s, the curve appears the maximum amplitude 1.08 meter; when the wave frequency is less than 1.4 rad/s, the BLDII curve keeps still, however, the change of heave RAO has a significant fluctuation in the range of 2.0~3.0 rad/s; and reaching 2.15 meter, the maximum amplitude, in 2.7rad/s of wave frequency. As BLDIII and IV, there is little change when the wave frequency is less than 1.6 rad / s; and also keep stable with the increase of wave frequency; But, BLDIV's heave RAO has a large changes in the range of 3.7~4.8 rad/s and it reaches a maximum, when wave frequency equal 4.4 rad / s.

Through comparative analysis we can find that in the range of low and part wave frequency, the heave RAO value of each BLD tends to 1meter, and gently changed with the increase of wave frequency; while in high and part wave frequency, heave RAO amplitude of BLDII is bigger and respond acutely, other buoys perform good. Hence, in terms of heaving RAO, the performance of BLDIII and IV are better, BLDI followed, and BLDII is the worst.

It can be indicated from Fig. 12 and 13 (roll and pitch RAO graph) that the RAO value of four BLD increase firstly and then decrease when reach up to one maximum in the roll DOF. As the wave angular frequency is less than 0.6rad/s, it has a small RAO value, and when the wave angular frequency beyond 3.8rad/s, BLDIII has the smallest RAO value. And BLDI, BLDII, BLDIII, BLDIV will gain their greatest value in 3.4rad/s, 2.8rad/s, 3.3rad/s as well as 3.3rad/s respectively. In terms of pitch RAO cure, BLDI, BLDIII, BLDIV are much same as the roll RAO curve, except that BLDII has a big difference. When the wave angular frequency is less than 1.0rad/s or more than 3.2rad/s, RAO value are

smaller and its curve changes slightly, and it turn to the maximum value at 1.8rad/s. BLDII has small response value of pitch RAO in high frequency (HF) and low frequency (LF) but great response in wave frequency.

As we can see from Fig. 14, with the increase of wave angular frequency, the yaw RAO value of each BLD rapidly reduce to zero. By comparison, the yaw RAO value of BLDIII is the smallest, BLDIV followed and BLDI is the largest one. Although BLDIII buoy structure is only symmetric about X axis, its yaw RAO value is still less than 0.4. On the whole, each buoy RAO response values are smaller.

After contrastive analysis, it can be concluded that before the RAO obtain extremum value, BLDIII and BLDIV's roll RAO curve change slowly that comparing with BLDI and BLDII. Concerning roll RAO extremum value, BLDI is the biggest, BLDII followed, as well as BLDIII and BLDIV are similar small ones, except that BLDIII becomes the smallest in partial HF. In pitch RAO value, BLDII is the biggest, BLDI followed, and the last two are BLDIII and BLDIV. Therefore, BLDIII and BLDIV perform well in roll and pitch RAO, while BLDI and BLDII behave relatively poor.

## 7 Short term forecast and calculation and relative analysis

Normally, waves in the real sea condition are random and irregular, so we should use Random-probability principle to calculate the motion response of buoy under the action of irregular Waves. By putting AQWA-FER model into use, ignoring the effect of wind and current, and using JONSWAP wave spectrum to calculate, among them, wave incident angle is 0°, 30°, 45°, 60° and 90° respectively. And then make a series of short-term forecast for the four BLDs, in the four degrees-of-freedom (yaw, roll, heave and pitch). The statistical result of short-term forecast ,including significant value and maximum value for the motion response amplitude of buoy. In the process of calculation, the significant wave height and wave period for Sea state conditions are 2.44m and 6.43s respectively.

Because of large numbers of the statistical date of the four BLDs under five different wave direction, this paper only choose five maximum value to show the cumulative results on table 4. And the significant amplitude of different BLDs is shown in figure 14 (among them, heave unit is "m", the other three's unit is "deg").

**Table 4** Four BLD's RAO results statistics

BLDI RAO results			
Motion	Sig Amp.	Max Amp.	Max wave direction
yaw	0.016	0.020	0°
heave	1.218	1.553	No effect
roll	14.930	19.036	90°
pitch	14.930	19.036	0°
BLDII RAO results			
yaw	18.533	23.630	60°
heave	1.270	1.619	Low effect
roll	15.053	19.193	90°
pitch	33.051	42.140	0°
BLDIII RAO results			
yaw	1.232	1.571	30°,90°
heave	1.200	1.530	Low effect
roll	10.337	13.180	90°
pitch	10.621	13.542	0°
BLDIV RAO results			
yaw	0.374	0.477	30°,60°
heave	1.195	1.524	Low effect
roll	10.336	13.178	90°
pitch	10.335	13.177	0°

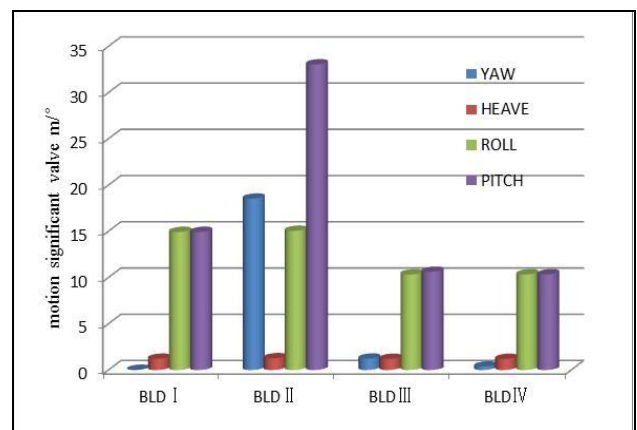


**Fig.15** RAO value comparison of each BLD

From table 4 and figure 15, we can find that the roll and pitch RAO maxima of four BLDs appear at the wave direction of 90° and 0° respectively, and the direction of waves has no

effect on heave RAO. At the same time, different BLD's yaw RAO maxima appears in different wave direction, because the four BLDs have great differences in structure. Concerning heave RAO, the significant and maximum amplitude value is 1.2m and 1.55m respectively, and they are similar to each other in value. In terms of roll RAO, BLDIII and BLDIV's significant and maximum amplitude value are around 10° and 13°, while BLDI and BLDII are around 15° and 19°. The pitch and roll RAO are broadly similar, whereas, BLDII's significant and maximum amplitude value vary widely that reached up to 33° and 42°.

We can concluded through relative analysis that in terms of pitch and roll RAO, BLDIII and BLDIV performed well with at least one-third smaller than that of BLDI and BLDII in value. As for heave RAO, all the four BLDs did well and had the similar statistics. In yaw RAO, besides BLDII the other three did a good job. So based on the short term forecast and the whole thing, BLDIII and BLDIV's RAO results are better.

## 8 Conclusion

This paper makes a brief introduction of the technical feature of FLB systems' solution, and based on this, we imitated four BLDs and made calculation of its intact stability, motion response as well as the short term forecast in the range of frequency domain. Through the summary and analysis of the results, we may draw a conclusion that:

(1) In the aspect of stability, BLD I , BLD II and BLDIII's specific stability parameter can meet the requirements of Regulation. The BLD IV needs extra adjustments on heeling angle for maximum righting lever. On the whole, composed of many separated small water-plane, multi-body combined buoy has a large waterplane moment of inertia and forms the advantage in stability over traditional single body buoy.

(2) Concerning heave, roll and pitch RAO graph, BLDIII and BLDIV had the outstanding performance and similar results in both RAO value and curve changes. While BLD I and BLD II 's results formed a great gap and disadvantages. Comparing with traditional single body buoy, the multi-body combined buoy's hydrodynamic characteristic did better and bear small differences in RAO.

(3) The changes of wave direction had a large effect on the roll and pitch RAO of buoy, It also had little influence on heave RAO. According to the structural type of different buoy, the changes

of wave direction will somehow effect yaw RAO. In the short term forecast that under a particular sea state, BLDIII and BLDIV were at least one-third smaller than BLDI and BLDII in roll and pitch RAO value, and the four BLDs had little difference on heave RAO value. While in terms of yaw RAO value, except BLDII has big RAO value, the other three hold small and similar values. Overall, the RAO performances of BLDIII and BLDIV that belong to multi-body combined buoy structural type are better.

(4) On the various performance indicators that need special attention and comparative analysis, BLDIII and BLDIV, multi-body combined buoy, do a good performance and show small gaps in value. Taking the cost of design & construction cost, the difficulty of installation & debugging and the convenience of transport & dismounting into account three-body combined buoy has more advantages over four-body combined buoy, so we can consider to use three-body combined buoy structure style for the design and exploitation of the new and professional floating LiDAR buoy system in the future.

The conceptual design and motion response analysis within the scope of time domain of three-body combined floating LiDAR buoy will be studied in the next stage. The popularization and application of floating LiDAR buoy system in offshore wind power industry also need to be considered in the future.

## Acknowledgements

I would like to express my deep appreciation to "scientific research innovation project for graduate student of Jiangsu province ordinary university" (YSJ15S-03), as well as Dr. Wei He from Statoil

## References

- CCS. 2005 Rules for Construction and Classification of Mobile Offshore Drilling Units, China communication press, Beijing.
- Jun-cheng Wang. 2013 Principle and Engineering of Ocean Data Buoy, The Ocean Publishing Company, Beijing, pp.121-122.
- M.Pitter, E.Burin des Roziers, et al. Performance stability of ZephIR in High Motion Environments, C.EWEA2014, Spain, 2014, 10), pp. 1-13.
- Pena.A., Hasager.C.B., Gryning.S, et al. Offshore wind profiling using light detection and ranging measurements, J.Wind Energy. 2009, 12(2), p.105-12



Yu Xiao-chuan, Xie yong-he, et al. The Influence of Water Depth on Motion Response and Wave Induced Loads of a Large FPSO, J. Journal of Shanghai Jiaotong University. 2005, 39(5), pp. 674-677.

Zhi-yi Liao, Heng-wen Zhang. The Application of Floating Lidar Wind Profiling System on Wind power, J. Journal of Mechatronic Industry, 2012,10(355), pp. 111-121.

Zhen-bang Sheng, Ying-zhong Liu. 2009 Principle of Ship, Shanghai Jiaotong University Press, Shanghai, pp.100-103.